Click Here for Full Article

# Heavy-tailed travel distance in gravel bed transport: An exploratory enquiry

K. M. Hill,[1] L. DellAngelo,[2] and Mark M. Meerschaert[3]

[1] Bed load transport, where particles move intermittently in frequent contact with the bed, is the dominant mode of particle transport in gravel bed rivers and streams. Complex fluid/particle and particle/particle interactions lead to a broad distribution of transport behaviors under the same set of flow conditions. In this paper, we investigate the plausibility of heavy-tailed movements for particles in bed load transport using carefully controlled flume experiments and theoretical analysis. In our experimental setting, we find travel distances for particles of a given size follow an exponential distribution whose mean varies with grain size. Building on previous work of Stark et al. (2009), we then develop a probability model to show how heavy-tailed distributions of travel distance can emerge from a mixture of particle sizes. Heavy-tailed travel distance can lead to anomalous diffusion in bed load transport, modeled by fractional derivatives in the transport equation.

## 1. Introduction

[2] Bed load transport is the dominant mode for particle transport in gravel bed rivers and streams and for the motion of smaller, sand-sized particles under lower flow conditions. As such, the prediction and understanding of bed load transport under various flow conditions is important for a broad array of problems, including river morphology, its evolution, and stream restoration. In contrast with the relative predictability of finer particles moving with the overlying fluid in suspension, the movement of particles in bed load transport takes place as a series of starts and stops. A particle at rest on the bed has a finite probability of becoming entrained into motion. Once a particle is entrained, its motion consists of a series of steps as the particle saltates, rolls, and/or slides in frequent contact with the bed, until it becomes distrained, and possibly buried beneath the surface [e.g., *Drake et al.*, 1988]. The complex movement arises from complicated fluid/particle and particle/particle interactions, which has hindered the development of a fully predictive model.

[3] Since *Shields* [1936] performed his classic experiments, there have been various attempts to model bed load transport. Historically, models developed for predicting average transport rate $\langle Q_b \rangle$ of particles in bed load transport have fit model parameters to field and laboratory flume data as a function of shear stress [e.g., *Meyer-Peter and Müller*, 1948; *Ashida and Michiue*, 1972; *Engelund and Fredsoe*, 1976; *Fernandez Luque and van Beek*, 1976; *Wong and Parker*, 2006]. Two methods for data acquisition are prominent. In the first method, all particles arriving at or crossing a line are recorded, often by catching particles arriving at a region of the bed using a device such as a Helley-Smith bed load sampler or a trap. In the second method, particles are painted (or labeled with other methods, e.g., through the use of radio-tracking devices, as in the work of *Habersack* [2001]) and placed in a bed, and their travel distances are measured after one or more transport events. Here we use travel distance to describe a displacement that can consist of multiple steps, even during a single transport event (e.g., flood). In both methods, typically an average displacement, effective velocity, and/or transport rate is computed and compared with average transport conditions such as shear stress. While these models often work well for the system in which they were derived, when taken out of this context the predictive power is somewhat limited. For example, when comparing their predictions for transport under the same flow conditions, they may differ from one another by orders of magnitude.

[4] Because of complex particle/particle and fluid/particle interactions, movement of particles in bed load transport is essentially stochastic. *Einstein* [1937, 1950] models the random motion of particles as intermittent movements, taking into account a fixed finite probability of particle entrainment at every time step. Once entrained, the particle moves a distance that scales with the size of the particle. Einstein's model for bed load transport treats these displacements as instantaneous and mutually independent, and models displacements with a gamma distribution [*Einstein*, 1937].

[5] More recent advances take into account duration of particle movement [*Lisle et al.*, 1998], correlated particle movements [*Ancey et al.*, 2008], turbulence statistics

[1]Saint Anthony Falls Laboratory, Department of Civil Engineering, University of Minnesota, Minneapolis, Minnesota, USA.
[2]Barr Engineering, Minneapolis, Minnesota, USA.
[3]Department of Statistics and Probability, Michigan State University, East Lansing, Michigan, USA.

[*Kleinhans and van Rijn*, 2002; *McEwan et al.*, 2004], and spatial [*Dancey et al.*, 2002] or temporal [*Wong et al.*, 2007] variability in bed elevation. *Kleinhans and van Rijn* [2002] use a probability distribution function (pdf) to model variability of bed shear stress due to turbulent fluctuations, and the resulting effect on particle transport. *McEwan et al.* [2004] invoke variations in critical shear stress within each size fraction to model variations in grain size distribution in bed load transport. The stochastic model of *Wong et al.* [2007] studies the link between temporal bed height fluctuations, hydraulic parameters, and vertical and streamwise displacements of tracer stones. Increased computer power has allowed the implementation of computationally intensive modeling techniques, such as the Discrete (or Distinct) Element Method (DEM) [*Cundall and Strack*, 1979], adapted for bed load transport and other aspects of sediment transport [*Heald et al.*, 2004; *Schmeeckle and Nelson*, 2003; *Gotoh and Sakai*, 1997; *Haff and Anderson*, 1993; *Drake and Calantoni*, 2001]. Recent technological developments allow these computational and theoretical models to be tested against high-resolution data [*Schmeeckle et al.*, 2007; *Papanicolaou et al.*, 2002].

[6] These models of bed load transport assume a thin-tailed pdf for travel distance or step length of individual particles (e.g., exponential, normal, lognormal, gamma). In a provocative new approach, *Ganti et al.* [2010] in this volume propose a heavy-tailed model for particle step length, and discusses the implications for long-term transport. Here a heavy tail means that the probability that a single particle travels a long distance in a single step falls off like a negative power of the step length. Based on a probabilistic Exner equation [e.g., *Parker*, 2008], they find that the long-time dynamics of particles with a thin-tailed step length are governed by the classical diffusion equation. For heavy-tailed step lengths, a fractional diffusion equation applies at late time. The fractional diffusion equation models anomalous diffusion, where particles spread faster than in the classical model [*Benson et al.*, 2000]. The underlying model of heavy-tailed particle motion is called a Lévy flight [*Weeks et al.*, 1998].

[7] There is some indirect evidence that bed load transport systems may exhibit power law statistics. Recent measurements by *Nikora et al.* [2002] have identified anomalous diffusion in some bed load systems. Average measured sediment transport rate can vary like a power law in the time interval over which the average is taken [*Singh et al.*, 2009; *Bunte and Abt*, 2005]. A theoretical discussion of *Stark et al.* [2009] and a related discussion of *Ganti et al.* [2010] illustrate how a power law pdf of step length for a mixture of grain sizes can result from a thin-tailed step length pdf for particles of a given grain size, combined via the pdf of grain sizes. That discussion will be revisited and expanded in section 4 of this paper, where we will also discuss the relation between step length and travel distance for heavy-tailed movements.

[8] In this article, we investigate the travel distance pdf of particles in bed load transport, both experimentally and theoretically, to determine the plausibility of a heavy-tailed pdf for particle step length. We conduct our experiments under lower-regime plane-bed equilibrium bed load transport conditions to eliminate variability associated with bed topography [*Haschenburger and Wilcock*, 2003]. We further minimize spatial variability in bed composition by using a gravel bed with a narrow distribution of grain sizes. This simplified experimental system will be described in detail in section 2. We monitor the displacements of particles as a function of size, and report our findings in section 3. In section 4, we consider a mix of particle sizes more typical of that found in the field, and discuss a probability model combining the travel distance pdf for any given grain size according to the pdf of grain sizes. That model explain how a power law pdf of travel distance can arise in practice. We also discuss, in that section, a simple relation between step length pdf and travel distance pdf that pertains in the heavy-tailed case. In section 5, we summarize the results of this paper, and discuss future challenges and opportunities.

## 2. Experimental Arrangement

[9] The experiments reported here were conducted in a 27.5 m long flume with a rectangular cross section 0.5 m wide × 0.9 m deep, operated with an erodible sediment bed and nonerodible walls (the "sediment flume" at St. Anthony Falls Laboratory at the University of Minnesota. Please see http://www.safl.umn.edu/facilities/facilities.html for more details). Sediment that traveled out of the flume was collected by a sediment trap and recirculated back to the upstream end of the flume. At this point, the sediment entered a separator box, and was refed into the flume at a constant predetermined rate, to create a sediment feed flume (see discussions of *Parker and Wilcock* [1993] and *Wong et al.* [2007]) where water discharge and sediment feed rate were controlled, so that bed slope and water flow depth evolved depending on these two parameters. As will be detailed below, the sediment size distribution was relatively narrow, and unchanged over the course of the experiments.

[10] To minimize complicating factors for this transport study, we operated the flume in lower-regime plane-bed equilibrium transport conditions, with a well-sorted gravel bed. The median grain size was $d_{50} = 7.1$ mm; the geometric mean particle size was $d_g = 7.2$ mm; the roughness height of the bed is indicated by $d_{90} = 9.6$ mm; the geometric standard deviation of the grain size distribution was 1.2, and the particle density was $\rho_s = 2550$ kg/m$^3$. Here $d_p$ denotes the $p$th quantile of the particle size pdf, so that $p$% of the particles have diameter less than or equal to $d_p$. (Here, as is customary, our pdf is according to particle weight, not number. See *Kellerhals and Bray* [1971] for discussion.) We used tracer particles primarily obtained from the bed using sieve sizes 4.0 mm, 5.6 mm, 6.3 mm, 8.0 mm, and 9.5 mm, though for sufficient quantities of the 9.5 mm particles we acquired some from other sources. Tracer particles are grouped by the largest sieve on which they were retained. Gravel tracers were colored using paint and permanent markers for easy identification, according to size and original placement in and on the bed.

[11] To bring the flume to steady state conditions (i.e., mobile bed equilibrium) prior to an experimental run set, a preparation time on the order of 50 h was needed, with water and sediment fed at a constant rate. The exact time depended on how close the prior flume conditions were to the desired conditions. During the first and longest part of this preparation, water and sediment were fed until the volume of sediment leaving the flume was equal to the sediment feed rate, verified by noting that the level in the separator box was unchanging. (This assumes the packing fraction in the box is

**Table 1.** Experimental Conditions for the Four Run Sets[a]

| Run Set | $Q_w$ (m³/s) | $Q_{bf}$ (m³/s) | $S_0$ (%) | $S_W$ (%) | $h$ (m) | $T_w$ (°C) | $t$ (s) | $\tau^*$ | GSD |
|---------|--------------|-----------------|-----------|-----------|---------|------------|---------|----------|-----|
| 1 | 0.0235 | 0.0075 | 1.29 | 1.28 | 0.070 | 10.0 | 240 | 0.0756 | mono |
| 2 | 0.0307 | 0.027 | 1.22 | 1.20 | 0.086 | 25.0 | 240 | 0.0900 | mono |
| 3 | 0.0415 | 0.064 | 1.15 | 1.15 | 0.10 | 8.0 | 240 | 0.101 | mono |
| 4 | 0.0307 | 0.027 | 1.22 | 1.20 | 0.086 | 25.0 | 240 | 0.0900 | mixed |

[a]Variable definitions are given in the text.

unchanging, which seems reasonable given that the conditions of particle entrance into and exit from the box are unchanging. Further, due to the narrow distribution of particle sizes in the bed and the lack of any streamwise segregation observed, we assume that the distribution of particle sizes leaving and entering the flume is relatively constant. For a wider distribution of particle sizes this may not be true and periodic sorting and weighing of the particles leaving the flume may be necessary to verify the steady state conditions.) To further assure the steady state of the system, longitudinal slopes of the bed surface and water surface were monitored to assure they remained relatively constant in time and space. Piezometers located every 0.5 m along the streamwise direction of the flume were used to measure water surface elevation along the flume. A point gauge was used to measure the longitudinal profile of the bed at three different transverse positions across the bed at every 0.5 m along the streamwise direction of the flume. The latter was used both to determine when the flume was at steady state and also to determine that there were no bed forms present. For all experimental results reported here, minimal or no bed forms were present during the run. For the experiments reported in this study, the minimum and maximum channel averaged flow velocities were 0.69 m/s and 0.9 m/s, respectively, and $d_{10} = 5.9$ mm, well within the range of lower-regime plane-bed conditions of *Southard* [1991].

[12] A summary of the average experimental parameter measurements for all runs sets discussed in this paper is presented in Table 1. Table 1 indicates water discharge $Q_w$, sediment feed rate $Q_{bf}$, experimental run duration $t$, temperature of the water $T_w$, water height above the weir $h$, nondimensionalized shear stress $\tau^*$, and particle size distribution in the tracer patches. Bed shear stress $\tau_b$ was nondimensionalized with the commonly used form:

$$\tau^* = \frac{\tau_b}{(\rho_s - \rho_w)gd_{50}} \quad (1)$$

in terms of the water density $\rho_w$, solid particle density $\rho_s$, gravitational acceleration $g$, and median grain size $d_{50}$. This nondimensionalized bed shear stress is also known as the Shields number [*Shields*, 1936]. In laboratory open channel flows, the bulk flow parameters are exposed to sidewall friction effects. We used the sidewall correction procedure introduced by *Vanoni and Brooks* [1957] to remove these sidewall effects. The run duration of 4 min was chosen to balance the number of moving particles with the number of particles exiting the end of the flume. The bed shear stresses were chosen to maintain plane bed conditions, taking into account the number of particles exiting the flume during the run. For the largest particles, at the smallest shear stress, ≈3% were entrained over the course of the experiment. At the largest shear stress, 30% of these particles exited the flume.

Using relations presented by *Parker et al.* [2003] and *Parker* [2008], we calculated that the range of dimensionless shear stress in this experimental set was 3–4 times the critical Shields stress, $\tau_{ci}^*$, for each size tracer particle.

[13] Experimental conditions in this study were comparable to bankfull conditions in several natural gravel bed streams [*Church and Rood*, 1983] (see Figure 1). The alluvial river channel data of *Church and Rood* [1983] were compiled from various sources on 284 streams and rivers. The data shown in Figure 1 only include gravel bed channels, with gravel or bedrock banks, and bed shear stresses at bankfull or 2 year recurrence interval flood discharge. The bed slopes for our experiments were somewhat steeper than those of *Church and Rood* [1983] for the same shear stress. However, both our bed slopes and dimensionless bed shear stress values lie well within the range of that data set.

[14] Once we verified a state of mobile bed equilibrium, we temporarily shut down the flume for the placement of tracer particles in several streamwise and transverse patches. The patches consisted of 2–3 layers of tracer particles (depending on the shear stress) to assure that all particles moving from a particular position in the flume could be monitored. As long as no particles from the bottom layer moved, we judged that all particles entrained from an initial location were accounted for. During our experiments, there was very little movement from any subsurface layer, even at the highest shear stress. To place the particles in patches, we first carefully excavated a small patch of particles with a surface area of 10 cm × 10 cm, to a depth of integral multiples of ~12 mm (to slightly exceed $d_{90}$), verified by surveying the excavated region with a point gage. The local patch of particles was replaced with an equal volume of tracer particles, in layers of thickness of ~12 mm. Each layer was leveled and surveyed with a point gage, so that the thickness of each layer was fairly uniform, and the top of the patch remained level with the surface of the bed. A simple schematic of the two-dimensional cross-sectional profile of a volume of planted tracer particles is shown in Figure 2.

[15] Once the tracers were placed, water and sediment feeds were restarted under equilibrium conditions established prior to the run. This start up was performed carefully, to minimize the effect of unsteady conditions during start up. The water
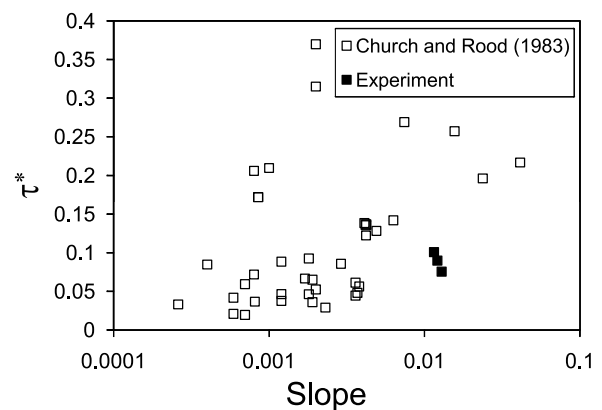


**Figure 1.** Shields stress ($\tau^*$) of 2 year recurrence interval and bankfull discharges of gravel bed streams as a function of channel slope for experiments presented in this paper (closed squares) and from the database of *Church and Rood* [1983] (open squares).
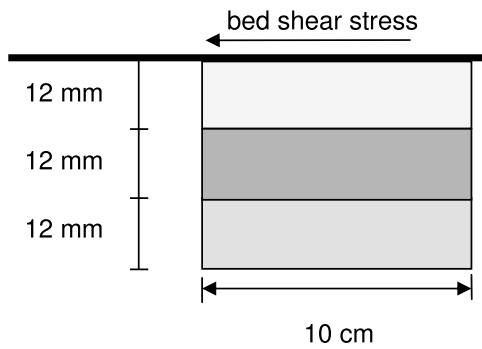
**Figure 2.** Schematic of the placement of tracer particles in layers.

feed was brought up slowly, until particles just barely started to move; then the sediment feed was started, and the water flow rate was brought rather quickly to that of steady state conditions. This last part typically took ~20–30s, or ~10% of the duration of our 4 min. runs. The "clock" was started when the water flow rate had reached steady state conditions. The flume ran for 4 min, and was then stopped. The 4 min duration was chosen so that, under the conditions imposed, most of the tracers stopped before reaching the end of the flume. The final locations of all tracer particles in the bed were recorded according to how far the particles traveled downstream, and whether or not they were buried beneath the surface. A maximum loss of 0.2% of tracer was recorded in our exper-

imental runs, so that essentially all of the tracer particles were recovered.

## 3. Experimental Results and Analysis

[16] In this section, we summarize the results from our flume experiment. Our focus is on the pdf of travel distance and how it relates to particle size. Prompted by these results, in section 4, we will develop a probability model of travel distance that pertains to a mixture of grain sizes using the data from the flume experiment.

### 3.1. Travel Distance pdf for Particles of a Given Size

[17] Figures 3, 4, and 5 show the relative frequency data for tracer particle travel distance for runs 1, 2, and 3, respectively. These runs are for mono-sized tracer particle patches. The shape of the data for all cases is similar, and resembles a gradual decay of probability with distance, with the shortest travel distances most likely. Several different alternative models were selected to fit the data for each particle size and shear stress, guided by previous literature. *Einstein* [1937] fit a gamma pdf to measured travel distance, and a Poisson distribution to resting times between movements. *Hassan et al.* [1991] also fit a gamma pdf to travel distance for a wide range of field data. We fit a Poisson distribution, a power law, a gamma, and an exponential to our measured travel distance. For our experimental data, we obtained a good fit with an exponential pdf:

$$f(x) = \lambda e^{-\lambda x} \qquad (2)$$
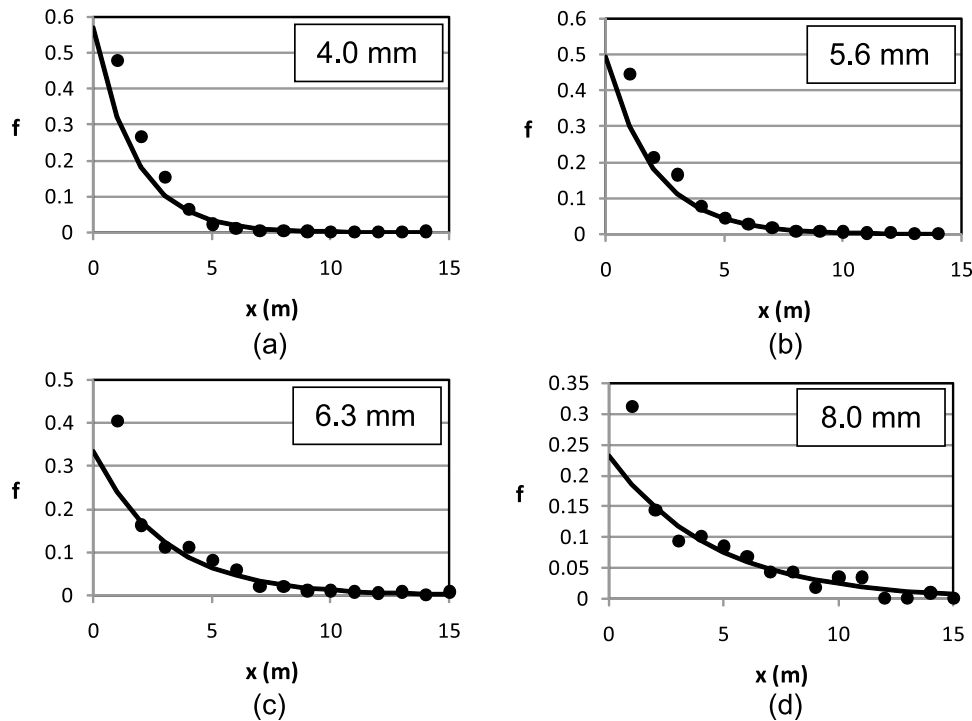


**Figure 3.** Plots showing empirical probability distribution functions of travel distances ($x$) for four different sized tracer particles during 4 min experiments. These plots contain particle travel distance data from run set 1 ($\tau^* = 0.076$). In each case, the solid line is the truncated exponential pdf $\lambda e^{-\lambda x}/[1 - \exp(-\lambda x_{max})]$ for the experimentally obtained data (points) for the tracers of sizes noted in an inset in each plot. In each case $x_{max}$ is taken as 15 m; $1/\lambda$ is plotted (as L) in Figure 8.
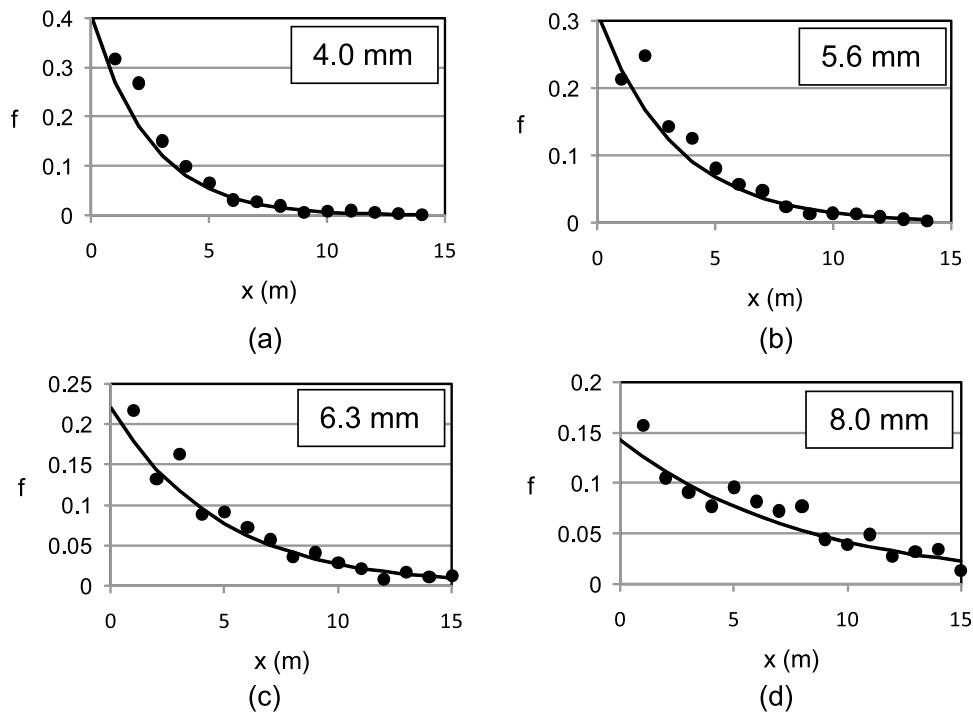
**Figure 4.** Empirical probability distribution functions of travel distances from run set 2 ($\tau^* = 0.090$). As in Figure 3 the results shown are the truncated exponential pdf $\lambda e^{-\lambda x}/[1 - \exp(-\lambda x_{max})]$ (solid line) for the experimentally obtained data (points) for the tracers of sizes noted in an inset in each plot.
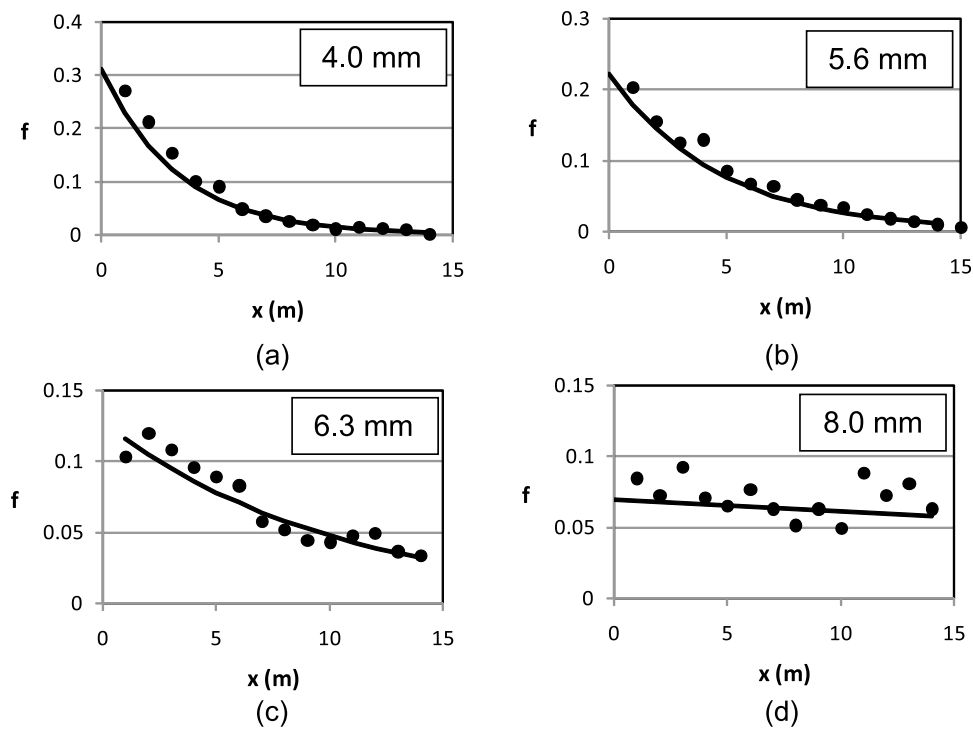


**Figure 5.** Empirical probability distribution functions of travel distances from run set 3 ($\tau^* = 1.01$). As in Figure 3 the results shown are the truncated exponential pdf $\lambda e^{-\lambda x}/[1 - \exp(-\lambda x_{max})]$ (solid line) for the experimentally obtained data (points) for the tracers of sizes noted in an inset in each plot.

(a)



(b)



(c)
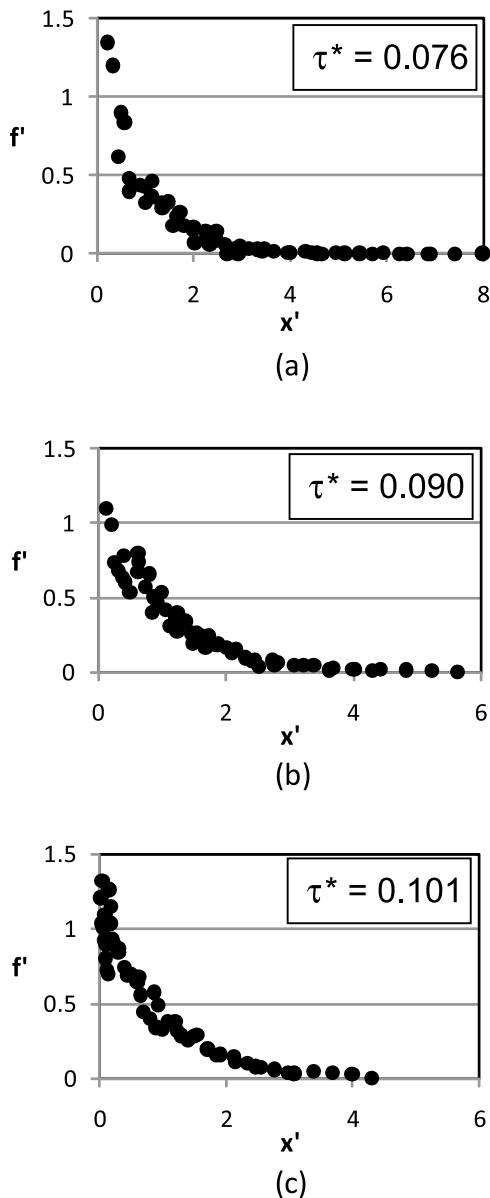
**Figure 6.** Results from the parametric collapse described in the text for the data shown in Figures 3–5, where $\tau^*$ is noted in the inset for each plot.

where $\lambda$ was treated as a fitting parameter, with units of 1/length. The exponential pdf fit significantly better than the Poisson distribution, and somewhat better than a power law, judged on the basis of mean squared error. A gamma distribution fit the data only marginally better than the exponential, and contains one additional fitting parameter. Therefore, we chose the exponential distribution in this study, for simplicity.

[18] Since our travel distance measurements are truncated due to finite flume length, we accounted for this in our fitting. In particular, we note that the data is cut off at some distance $x_{max}$, which we take to be the maximum observed travel distance for each case. The truncation effect is negligible in most cases, but significant in cases like Figure 5d, where a significant number of particles exited the flume, and the resulting graph does not tend to zero as observed travel dis-

tance increases. We fit the exponential pdf to the observed travel distance data as follows. After determining the fraction $f_i$ of particles that travel a distance $x_i$, we considered a theoretical pdf $f(x)$ given by equation (2), and chose the fitting parameter $\lambda$ to minimize the sum of squared errors:

$$\sum_i \left( f_i - \frac{f(x_i)}{1 - \exp(-\lambda x_{max})} \right)^2 \tag{3}$$

where the denominator

$$1 - \exp(-\lambda x_{max}) = \int_0^{x_{max}} f(y)\, dy$$

corrects for the truncation. If $X$ denotes travel distance, then the fraction in (3) represents the conditional density of $X$ given $X < x_{max}$. Based on this fitting procedure, the resulting exponential pdf for each case was plotted against the data in Figures 3, 4, and 5.

[19] It is reasonable to ask why the exponential pdf might fit these data, and whether some plausible probability model for the underlying motions could lead to an exponential pdf for travel distance. Travel distance is composed of some unknown random number of step lengths, representing the number of entrainments of a particle. The theory of random sums shows that, for any step length pdf with a finite mean, a geometric random number $N$ of steps with $P(N = n) = p(1 - p)^{n-1}$ for some $0 < p < 1$ and $n \geq 1$, will result in an overall travel distance that is approximately exponential [Kotz et al., 2001, p. 30]. Indeed, if the step length is exponential, and the number of steps is geometric, then the travel distance is also exponential. Geometric sums occur frequently in applications to physics, biology, economics, and insurance mathematics [Kalashnikov, 1997]. It would be interesting to investigate the underlying model further, especially if one could gather appropriate data on the number of entrainments (e.g., using radio-tagged particles).

[20] To further test the exponential model of travel distance pdf, we performed a similarity collapse for each experimental Shields stress using the mean travel distance $L = 1/\lambda$, in the following manner. The pdf of travel distance $f(x)$ is approximated by data in Figures 3, 4, and 5. Let $x_i$ denote distance and $f_i$ the corresponding fraction of particles that traveled this distance. The data points $(x_i, f_i)$ were plotted in Figures 3, 4, and 5. Since the exponential fit to the random travel distance $X$ has mean $L$, the rescaled travel distance $X' = X/L$ has mean 1. The density of $X'$ is $f'(x) = Lf(Lx)$. This is approximated by a plot with value $f_i' = Lf_i$ at location $x_i' = x_i/L$. Expanding the heights while contracting the spacings by the same factor preserves the area (probability) under the curve. The results from this similarity collapse are shown in Figure 6. It appears that the fit is quite good, providing additional evidence in favor of an exponential travel distance pdf for particles of any given grain size in our experiment.

[21] As further verification, we tested the exponential fit using standard statistical tools. Figure 7 shows a probability plot comparing the raw data summarized in Figure 5a with the best fitting exponential distribution, found by the method of maximum likelihood. The fitted parameter by maximum likelihood is $\lambda = 0.34$, which is close to the value of $\lambda = 0.36$ obtained by least squares. A good fit is indicated if the data follow the reference line (quantiles of the theoretical pdf).
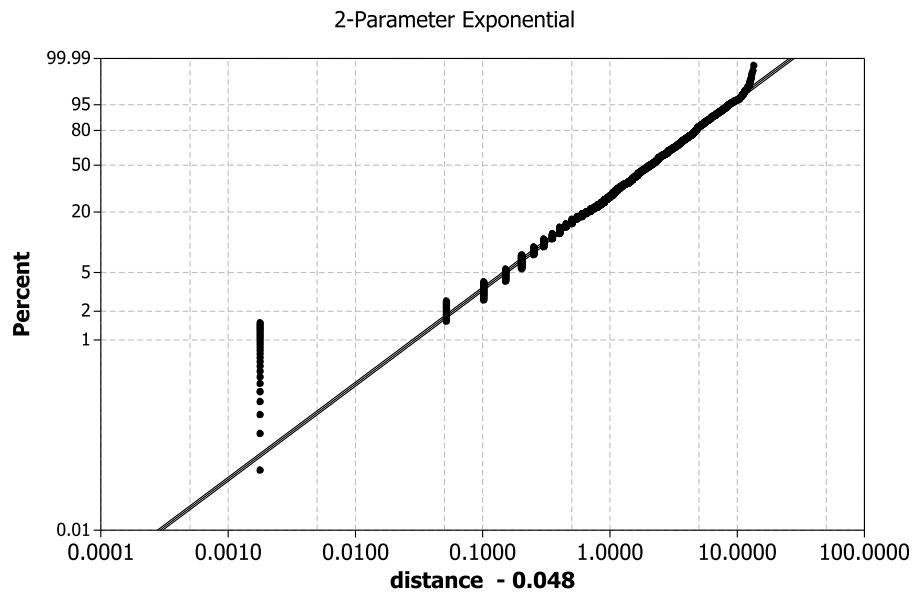
**Figure 7.** Probability plot for the data in Figure 5a compared to the best fitting exponential pdf model. Data is shifted slightly to obtain the best fit.

Here the fit is excellent. The lack of fit on the left is due to the resolution of the measurements (all these data values equal 0.05). To improve the fit in this high-resolution method, we allowed a small shift in the data, less than the granularity of the data. The optimal shift is 0.048, as shown in Figure 7. A slight lack of fit on the right is due to truncation effects (finite flume size). A more sophisticated fitting by maximum likelihood would take into account the truncation. A similar fitting for truncated power law data was recently accomplished by *Aban et al.* [2006]. It would be interesting to extend this approach to truncated exponential data.

[22] We also examined the travel distance data for particles found buried in the bed, versus those found on the surface (not shown). Both follow roughly the same shape as the combined data. Smaller particles were buried at a somewhat higher rate than larger particles. Further, for higher shear stress, the burial rate was higher for all transported particles. This suggests that some kinetic sieving occurred, with smaller particles more likely to find holes in which they can rest for longer periods. Burial statistics are related to waiting times between transport events [*Schumer and Jerolmack*, 2009; *Ganti et al.*, 2010] which in turn can affect both average transport and diffusion. In this paper, we investigate the relation between particle size distribution and displacement statistics, leaving a full investigation of burial rates and their impact on transport as an interesting direction for future research.

[23] In summary, we conclude that travel distances *for single-sized particles* can be accurately characterized by an exponential pdf, equation (2), with a rate parameter $\lambda$ that varies with particle size and experimental flow conditions, especially shear stress. However, typically there is a distribution of particle sizes in the field, and associated mixing over different particle sizes tends to broaden the distribution of travel distance. To see the form this may take, we need to consider how the travel distance pdf varies with particle size, and then how particle size varies in the field. Hence in section 3.2 we study the dependence of mean travel distance

$1/\lambda$ on grain size, and then in section 4 we investigate the impact of a mixture of grain sizes on the overall pdf of travel distance for particles of all sizes.

### 3.2. Size Dependence of Average Travel Distances

[24] In section 3.1 we found that travel distance for a given grain size and shear stress follows an exponential distribution whose pdf, equation (2), depends on the parameter $\lambda$. Of course the best fitting $\lambda$ varies with particle size and shear stress. Here we investigate the relation between travel distance and particle size. For readability, it is simplest to focus on the mean travel distance $L = 1/\lambda$, which is measured in the same units (m) as the data.

[25] Figure 8 shows the mean travel distance $L = 1/\lambda$ determined from the best exponential fit to each data set in Figures 3, 4, and 5, for each particle size. For the small range
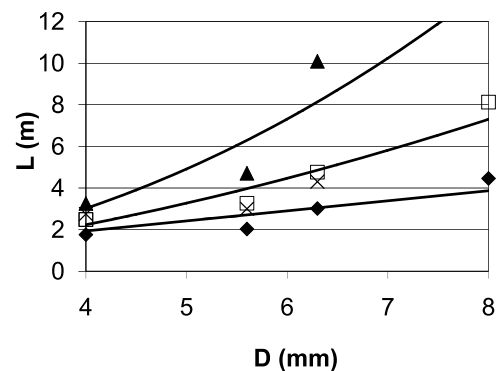


**Figure 8.** Mean travel distance $L$ (in meters) as a function of tracer particle size $D$ (in mm) along with the regression model $L = kD^q$ for each Shields stress: $\tau^* = 0.076$ (diamonds), $\tau^* = 0.090$ (squares), and $\tau^* = 0.101$ (triangles). Fitted values of $k$ and $q$ are given in the text. We also show mean travel distance for set 4 (crosses), with a narrow mixture of grain sizes used.

of shear stresses examined in our simple system, the mean travel distance increases with increasing particle size $D$. Note that the results obtained using patches of a relatively narrow distribution of different grain sizes, run set 4, is similar to the results obtained using patches of mono-sized grains under the same conditions, run set 2.

[26] Next we consider the functional relation between average travel distance $L$ and particle size $D$. In the existing literature, a linear relation between grain size and mean travel distance was reported by *Tsujimoto* [1978], while a nonlinear relation we found to be more representative in the works of *Church and Hassan* [1992] and *Ferguson and Wathen* [1998]. There are a number of differences between the two sets of data, including the steadiness in the flow. Motivated by this, we consider both a linear relation $L = cD$ and a power law relation $L = kD^q$ where $q > 0$, and plot the best fits in Figure 8. For all sets, a power regression gives the better fit. For set 1 ($\tau^* = 0.076$) a power regression $L = kD^q$ with $k = 0.240$ and $q = 1.36$ provides the best fit, with $R^2 = 0.88$ indicating an adequate fit. For set 2 ($\tau^* = 0.090$) a power regression $L = kD^q$ with $k = 0.209$ and $q = 1.71$ provides the best fit, with $R^2 = 0.92$. For set 3 ($\tau^* = 0.101$) a power regression with $k = 0.147$ and $q = 2.18$ gives the best fit with $R^2 = 0.80$. For case 3 we did not include the largest grain size (8.0 mm) in the regression, since the scatter in the data and the relatively lower fitted value of $\lambda$ rendered the estimated mean travel distance somewhat unreliable. If that point is included, we find $k = 0.0048$, $q = 4.37$ and $R^2 = 0.81$ in the resulting power law trend line. We note that the parameter $q$ increases with shear stress.

[27] In our experiments, larger particles travel farther than small particles, once entrained. While not common, this is not a unique observation. Similar observations have been documented in the field and laboratory by a number of authors [*Brummer and Montgomery*, 2003; *Tsujimoto*, 1978; *Straub*, 1935; *Kodama et al.*, 1992]. For example, *Brummer and Montgomery* [2003] found larger particles travel farther than small particles in the field in steep sediment transport systems, and *Miller and Byrne* [1966] found this to be true in debris fields. However, observations such as these have been rare [*Solari and Parker*, 2000]. Empirical relations for mean travel distance as a function of particle size vary across the literature. *Einstein* [1937] found a wide range of travel distances but no clear relation between travel distance and particle size in flume studies. *Hassan et al.* [1991] and *Ashworth and Ferguson* [1989] found similar results in natural rivers using tracer particles. Most natural rivers and streams exhibit downstream fining which, in some cases, seems to be driven by size-dependent particle mobility [*Paola et al.*, 1992]. *Church and Hassan* [1992] compiled data from a number of tracer particle studies in streams and rivers, and found mean travel distance decreases with particle size as a general rule. *Ferguson and Wathen* [1998] drew similar conclusions. *Solari and Parker* [2000] found they could control which particles traveled farther in their flume experiments by varying the slope. In their system, large particles traveled farther, a phenomenon they referred to as "reverse mobility," when the slope was sufficiently high. They argued that this can happen when a steep slope enables large particles to roll more easily out of a local pocket. *Solari and Parker* [2000] showed that, in their system, mobility reversal occurred at

slopes above 0.02–0.03. *DellAngelo* [2007] found that, in a more well-sorted system, the predicted reversal point occurs at even flatter slopes, consistent with the experimental results reported here. Another possible explanation for reverse mobility involves the point of distrainment rather than entrainment and the relative roughness of the bed. Finer particles "see" a rougher bed, relative to their size. This could cause larger particles, once entrained, to roll farther along the bed.

[28] In summary, we find that in our experimental setup, travel distance for particles of a given size follow an exponential distribution, where the mean travel distance increases like a power law function of the grain size. Other studies report a decrease in mean travel distance with grain size. Section 4 develops a probability model to explain how a typical mix of particle sizes found in the field can broaden the travel distance pdf. There we consider a general model $L = kD^q$ where large particles travel farther, as in our study, as well as an alternative (downstream fining) model $L = k/D^q$ where smaller particles travel farther. In both cases, it turns out that a typical pdf of grain sizes can sometimes lead to heavy-tailed particle motions.

## 4. Theoretical Discussion

[29] In section 3 we found that, for a particular Shields stress and particle size, the travel distance of a given particle during the course of our experiment follows an exponential pdf, equation (2). Thus the probability that a particle of size $D$ travels farther than a distance $x > 0$ downstream is given by

$$P(X > x | D) = \int_x^\infty L^{-1} e^{-y/L} dy = e^{-x/L} \qquad (4)$$

where the mean travel distance $L$ depends on the particle size, and $y$ is a dummy variable standing in for travel distance $x$ in the integral. In this section, prompted by the experimental results in section 3, we will construct a probability model to determine the effect of grain size mixtures on travel distance. This depends on two ingredients: the relation between mean travel distance $L$ and grain size $D$; and the pdf of grain sizes. Our model shows how a heavy-tailed pdf of travel distance for a mixture of grain sizes could emerge under natural conditions. At the end of this section, we will consider the implications for particle transport, based on the model of *Ganti et al.* [2010]. At that point, we will also discuss the relation between travel distance and step length in the case of heavy-tailed movements.

[30] Denote by $g(r)$ the pdf of grain size $D$, so that $P(D = r) = g(r)dr$. Then, using equation (4) along with the law of total probability, we can write the probability that a particle travels farther than a distance $x > 0$ downstream as

$$P(X > x) = \int_0^\infty P(X > x | D = r)g(r)dr = \int_0^\infty e^{-x/L} g(r)dr \quad (5)$$

In order to determine the (unconditional) probability distribution of travel distance from equation (5), it is necessary to substitute the model of mean travel distance $L$ as a function of grain size, as well as the pdf of grain sizes, and then analyze

the resulting integral. A power law distribution of travel distance can emerge under appropriate conditions.

[31] Many authors [e.g., *Wilcock and Southard*, 1989; *Garcia*, 2008; *Lanzoni and Tubino*, 1999; *Parker*, 2008] have used a lognormal PDF for grain size

$$g(r) = \frac{1}{r\sigma\sqrt{2\pi}} e^{-\frac{1}{2}\frac{(\ln r - \mu)^2}{\sigma^2}} \tag{6}$$

where $\mu$, $\sigma$ are the mean and standard deviation of the normal random variable $\ln D$. In this case, the overall (unconditional) travel distance distribution is given by

$$P(X > x) = \int_0^\infty e^{-x/L} \frac{1}{r\sigma\sqrt{2\pi}} e^{-\frac{1}{2}\frac{(\ln r - \mu)^2}{\sigma^2}} dr \tag{7}$$

but this integral is challenging. *Stark et al.* [2009] suggest the gamma pdf

$$g(r) = \frac{\beta^\alpha}{\Gamma(\alpha)} r^{\alpha-1} e^{-\beta r} \tag{8}$$

as a possible alternative with similar shape characteristics. In this case, assuming the simple model $L = k/D$, the integral (5) can be computed explicitly to reveal a power law tail for travel distance:

$$\begin{aligned} P(X > x) &= \int_0^\infty e^{-xr/k} \frac{\beta^\alpha}{\Gamma(\alpha)} r^{\alpha-1} \exp(-\beta r) \, dr \\ &= \left(1 + \frac{x}{k\beta}\right)^{-\alpha} \end{aligned} \tag{9}$$

as $x \to \infty$. Furthermore, it is not necessary that $g(r)$ be a gamma pdf, only that the behavior of the pdf near zero is asymptotically a power law. Moreover, a power law pdf for travel distance can emerge if we assume that smaller particles travel farther (downstream fining) according to the more general model $L = k/D^q$ for any $q > 0$. For mathematical details, see Appendix A.

[32] *Ganti et al.* [2010] consider a simple alternative model $L = kD$ for the case when larger particles travel farther, consistent with the experimental results of section 3. In that case, *Ganti et al.* [2010] use an inverse gamma pdf of grain sizes and a change of variables $y = 1/r$ in equation (5) to compute

$$\begin{aligned} P(X > x) &= \int_0^\infty e^{-x/kr} \frac{\beta^\alpha}{\Gamma(\alpha)} r^{-\alpha-1} \exp\left(-\frac{\beta}{r}\right) dr \\ &= \int_0^\infty e^{-xy/k} \frac{\beta^\alpha}{\Gamma(\alpha)} y^{\alpha-1} \exp(-\beta y) \, dy \\ &= \left(1 + \frac{x}{k\beta}\right)^{-\alpha} \end{aligned} \tag{10}$$

using equation (9). Assuming, more generally, that larger particles travel farther according to the model $L = kD^q$ for any $q > 0$, a power law travel distance pdf emerges whenever the grain size pdf follows a power law at large grain sizes, see Appendix A for details.

[33] In conclusion, a heavy-tailed power law pdf for travel distance can emerge when particles of a given size travel an exponential distance downstream, and a mixture of grain sizes pertains. Given a power law model for the mean travel distance $L$ as a function of the grain size $D$, the heavy tail results from the influence of particles that travel farthest. With

a downstream fining model $L = k/D^q$ where small particles travel farther, a heavy-tailed pdf of travel distance emerges if the pdf of small grain sizes follows a power law. With the alternative model $L = kD^q$ where large particles travel farther, as found in our experiments reported in section 3, a heavy-tailed pdf of travel distance emerges if the pdf of large grain sizes follows a power law. Of course it is possible that neither situation occurs, in which case the overall pdf of travel distance for a mixture of grain sizes could follow some light-tailed pdf, e.g., the normal distribution.

[34] *Ganti et al.* [2010] in this volume discuss the implications of power law step lengths for bed load particle transport. In short, a step length $S$ that satisfies $P(S > x) \approx Cx^{-b}$ for $x$ large can result in anomalous superdiffusion at late time, in which sets of particles diverge from one another faster than the classical diffusion model predicts. The nature of this spreading can be captured by an anomalous diffusion equation that employs a fractional derivative of order $1 < b < 2$ in place of the usual second derivative [*Benson et al.*, 2000]. This can affect sediment transport in ways that are still being investigated, including the rate and nature of size segregation, and bed topography.

[35] While *Ganti et al.* [2010] build on the pdf of step length, our experimental results measure the pdf of travel distance. Indeed, it is not easy to distinguish individual steps in the naturally stochastic and intermittent system of bed load transport. Fortunately, there is a mathematical result [*Kozubowski et al.*, 2003, theorem 4.1] which guarantees that, under the modeling assumptions of *Ganti et al.* [2010], a power law step length pdf leads to a power law travel distance, and vice versa. Specifically, when we add a random number of power law steps, and assuming that the random number of steps has a finite mean, the resulting travel distance has the same power law character as the individual steps, with the same power law index. In the work of *Ganti et al.* [2010] the number of steps in a fixed finite time interval (in section 3 the time interval was fixed at 4 min) has a Poisson distribution. Then the results of this section can be used to determine when the anomalous diffusion model of *Ganti et al.* [2010] is in effect. For a downstream fining system in which the mean travel distance for particles of diameter $D$ is given by $L = k/D^q$, the tail estimate in equation (A4) shows that anomalous diffusion pertains when $1 < \alpha/q < 2$, if the cdf of small grain sizes follows a power law with index $\alpha$ near the origin (or, equivalently, the pdf follows a power law with index $\alpha - 1$). For a system in which the mean travel distance for particles of diameter $D$ is given by $L = kD^q$, anomalous diffusion pertains when $1 < \alpha/q < 2$ if the cdf of large grain sizes follows a power law with index $-\alpha$ near infinity (or, equivalently, the pdf follows a power law with index $-\alpha - 1$). Given this result, and the profound implications of anomalous transport on the evolution of bed load transport, it becomes very important to develop better models and collect higher-resolution data on the grain size distribution in natural systems. For this purpose, a simple sieving method provides insufficient resolution to distinguish between power law and other distributional forms.

## 5. Conclusions

[36] We have presented the results from a controlled experimental study of gravel particles in bed load transport

through a gravel bed flume in the plane bed equilibrium transport regime. We have shown that the transport distance for particles of a given size follows an exponential pdf whose mean varies with particle size and experimental conditions, most notably shear stress. We have also developed a probability model to explain how, if these experimental results are extended to a system with a typical grain size distribution, travel distance of all particles can have a heavy, power law probability tail. In our experiments, larger particles are found to travel farther, a phenomenon termed reverse mobility by *Solari and Parker* [2000]. More commonly, smaller particles travel farther (downstream fining). In either case, our probability model indicates that a heavy-tailed pdf of travel distance can pertain to a mixture of grain sizes. This result suggests that power laws could emerge in many typical experimental or natural settings, related to familiar distributional models. As detailed in a separate paper in this volume [*Ganti et al.*, 2010], this wide distribution of particle displacements can lead to anomalous diffusion of particles downstream, when particles spread faster and farther than the classical diffusion model predicts. The model of *Ganti et al.* [2010] is based on step length, while we measure travel distance. However, under the model assumptions of *Ganti et al.* [2010], we argue that power law travel distance implies power law step length, and vice versa.

[37] Clearly, there are additional questions to be addressed, and we intend our results to motivate further study. This experimental study uses a fairly narrow set of particle sizes. While a narrow size distribution may occur in limited settings such as very short well-sorted reaches of gravel bed rivers or gravel patches along river beds, particle size distributions over a longer river reach in the field are broader. In these cases, predicting transport is further complicated by sorting of particles [see, e.g., *DellAngelo*, 2007; *Paola and Seal*, 1995; K. Hill et al., Mobility reversal, particle size distribution, and slope, manuscript in preparation, 2010]. Additionally, under different flow conditions, the bed morphology may be variable and include relief, for example in the form of bars and dunes. Even under the simplest conditions, prediction of particle transport should consider the possible effects of power law distributions. The data and theory presented herein provide a framework for addressing additional complicating effects that may exist in other flume studies and in the field.

[38] A central finding of this paper is a probability model that explains how power laws can emerge from an exponential travel distance pdf for particles of a given grain size, combined with a typical pdf of grain sizes in natural systems. Power laws emerge when the portion of the grain size pdf with the longest mean travel distance has a power law character. For example, in a system with downstream fining, where smaller particles travel farther, power laws emerge if the grain size pdf follows a gamma distribution, or a Weibull distribution, or a beta distribution. Hence the appearance of power law distributions of particle displacements in sediment transport is completely consistent with previous theory and experimental data. Certainly there is a need for additional research to investigate the possibility of power law statistics in natural and laboratory systems. We also note that it may be possible to infer power law behavior indirectly from measurements such as sediment load and bed topography. In the same spirit, the paper of *Schumer and Jerolmack* [2009]

in this volume considers evidence for power law waiting time statistics in the geological record. Further experimental research, and model development, seems warranted to investigate these issues.

## Appendix A: Travel Distance Distributions for a Mix of Particle Sizes

[39] In this appendix, we provide mathematical details to argue that a power law pdf of travel distance, for a mixture of grain sizes, can emerge from an exponential pdf of travel distance for grains of a given size $D$, combined according to an appropriate pdf of grain sizes. We begin with the unconditional probability that a particle travels farther than a distance $x > 0$ downstream, given by equation (5) in terms of the pdf of grain size, $g(r)$, and the mean travel distance $L$ for particles of a given size. To show that this expression can exhibit power law behavior, it is useful to apply Karamata's Tauberian Theorem [*Feller*, 1971, theorem 3, p. 445]. Write the cumulative distribution function (cdf) of grain sizes

$$G(x) = \int_0^x g(r)\, dr$$

so that $G(x) = P(D \le x)$. Denote the Laplace transform of the density $g(r)$ by

$$\tilde{g}(s) = \int_0^\infty e^{-sr} g(r)\, dr$$

Karamata's Tauberian theorem states that

$$\tilde{g}(s) \sim Cs^{-p} \quad \text{as } s \to \infty \quad \Longleftrightarrow \quad G(x) \sim \frac{Cx^p}{\Gamma(p+1)} \quad \text{as } x \to 0 \tag{A1}$$

Here we assume $p \ge 0$, and $g_1(x) \sim g_2(x)$ means that the ratio $g_1(x)/g_2(x) \to 1$. For example, $x^2 + 3x \sim x^2$ as $x \to \infty$, since the linear term is negligible compared to the $x^2$ term for large values of $x$. The essential reasoning behind (A1) is that letting $s \to \infty$ in the exponential term $e^{-sx}$ can be balanced by letting $x \to 0$.

[40] Equation (9) shows that, when $g(r)$ follows the gamma pdf in equation (8), and the average travel distance $L$ is related to the grain size $D$ by $L = k/D$, the expression in equation (5) can be explicitly computed to show that the probability of a travel distance greater than $x$ falls off like $x^{-\alpha}$ where $\alpha$ is the shape parameter of the gamma pdf. Alternatively, we can use equation (A1) to obtain the same asymptotic result. Since $e^{-\beta r} \sim 1$ for $r \to 0$ the gamma cdf satisfies

$$G(x) = \int_0^x \frac{\beta^\alpha}{\Gamma(\alpha)} r^{\alpha-1} e^{-\beta r}\, dr$$
$$\sim \int_0^x \frac{\beta^\alpha}{\Gamma(\alpha)} r^{\alpha-1}\, dr$$
$$= \frac{\beta^\alpha}{\Gamma(\alpha)} \frac{x^\alpha}{\alpha} = \frac{\beta^\alpha x^\alpha}{\Gamma(\alpha+1)} \quad \text{as } x \to 0$$

Then equation (A1) implies that

$$P(X > x) = \tilde{g}(x/k) \sim \beta^\alpha (x/k)^{-\alpha} \quad \text{as } x \to \infty \tag{A2}$$

Furthermore, it is not necessary that $g(r)$ be a gamma pdf, only that the behavior of the pdf near zero is asymptotically a

power law. For example, if we use a Weibull distribution with the model $L = k/D$, then

$$G(x) = 1 - \exp(-(x/\beta)^\alpha) = 1 - (1 - (x/\beta)^\alpha + \cdots) \sim (x/\beta)^\alpha$$

as $x \to 0$

and we immediately conclude from (A1) that

$$P(X > x) = \tilde{g}(x/k) \sim \Gamma(\alpha + 1)(x/k\beta)^{-\alpha} \quad \text{as } x \to \infty$$

For a beta distribution

$$G(x) = \int_0^x \frac{\Gamma(\alpha + \beta)}{\Gamma(\alpha)\Gamma(\beta)} y^{\alpha-1}(1 - y)^{\beta-1} \, dy$$

$$\sim \int_0^x \frac{\Gamma(\alpha + \beta)}{\Gamma(\alpha)\Gamma(\beta)} y^{\alpha-1} \, dy$$

$$= \frac{\Gamma(\alpha + \beta)}{\Gamma(\alpha + 1)\Gamma(\beta)} x^\alpha \quad \text{as } x \to 0$$

and then (A1) implies that

$$P(X > x) = \tilde{g}(x/k) \sim \frac{\Gamma(\alpha + \beta)}{\Gamma(\beta)}(x/k)^{-\alpha} \quad \text{as } x \to \infty$$

[41] More generally, if we assume that smaller particles travel farther (downstream fining) according to the model $L = k/D^q$ for some $q > 0$, then any grain size cdf with $G(x) \sim Cx^p$ as $x \to 0$ leads to a power law. To see this, let $Y = D^q$ so that $F(y) = P(Y \leq y) = P(D^q \leq y) = G(y^{1/q})$. Now $f(y) = F'(y) = g(y^{1/q})y^{-1+1/q}/q$. Then equation (5) and a substitution $y = r^q$ leads to

$$P(X > x) = \int_0^\infty e^{-xr^q/k} g(r) \, dr$$

$$= \int_0^\infty e^{-xy/k} f(y) dy$$

$$= \tilde{f}(x/k)$$

and, since $F(y) = G(y^{1/q}) \sim Cy^{p/q}$ as $y \to 0$, equation (A1) yields

$$P(X > x) \sim \Gamma(1 + p/q)C(x/k)^{-p/q} \quad \text{as } x \to \infty \qquad \text{(A3)}$$

For example, if the grain size follows a gamma pdf, and if mean travel distance is related to grain size by $L = k/D^q$, then we find a power law distribution of travel distance with

$$P(X > x) \sim \frac{\Gamma(1 + \alpha/q)}{\Gamma(1 + \alpha)} \beta^\alpha (x/k)^{-\alpha/q} \quad \text{as } x \to \infty \qquad \text{(A4)}$$

Here the power law tail index $\alpha/q$ depends on both the grain size pdf and the model for mean travel distance.

[42] For the simple alternative model $L = kD$ when larger particles travel farther, equation (10) shows that the probability of a travel distance greater than $x$ falls off like $x^{-\alpha}$ when $\alpha$ is the shape parameter of the inverse gamma pdf for particle size. Again, we may invoke equation (A1) to obtain the same asymptotic result. First we generalize to the model $L = kD^q$ used in section 3. Now any grain size cdf with $1 - G(x) \sim Cx^{-p}$

as $x \to \infty$ leads to a power law. To see this, let $Y = D^{-q}$ so that $F(y) = P(Y \leq y) = P(D^{-q} \leq y) = 1 - G(y^{-1/q})$. Now $f(y) = F'(y) = g(y^{-1/q})y^{-1-1/q}/q$ and equation (5) along with a substitution $y = 1/r^q$ leads to

$$P(X > x) = \int_0^\infty e^{-x/kr^q} g(r) \, dr$$

$$= \int_0^\infty e^{-xy/k} f(y) dy$$

$$= \tilde{f}(x/k)$$

and, since $F(y) = 1 - G(y^{-1/q}) \sim Cy^{p/q}$ as $y \to 0$, equation (A1) yields

$$P(X > x) \sim \Gamma(1 + p/q)C(x/k)^{-p/q} \quad \text{as } x \to \infty \qquad \text{(A5)}$$

For example, if the grain size follows an inverse gamma pdf, and if mean travel distance is related to grain size by $L = kD$, then

$$1 - G(x) = \int_x^\infty \frac{\beta^\alpha}{\Gamma(\alpha)} r^{-\alpha-1} \exp\left(-\frac{\beta}{r}\right) dr$$

$$\sim \int_x^\infty \frac{\beta^\alpha}{\Gamma(\alpha)} r^{-\alpha-1} \, dr$$

$$= \frac{\beta^\alpha}{\Gamma(\alpha)} \frac{x^{-\alpha}}{\alpha} = \frac{\beta^\alpha x^{-\alpha}}{\Gamma(\alpha + 1)} \quad \text{as } x \to \infty$$

and we find the same power law distribution of travel distance as for the gamma pdf with the downstream fining model (equation (A4) with $q = 1$). This is no coincidence, but rather a result of the fact that, if $D$ has a gamma pdf, then $D^{-1}$ has an inverse gamma pdf.

## Notation

$c$   fitting parameter used in linear regression between $L$ and $D$.
$C$   theoretical fitting parameter used in exponential particle size cdf.
$D$   particle size.
$d_p$   $p$th quantile of the particle size pdf ($p$% of the particles have diameter $d \leq d_p$).
$f_i$   size fraction $i$.
$g$   gravitational acceleration.
$g(r)$   pdf of grain size distribution.
$\tilde{g}(s)$   Laplace transform of $g(r)$.
$G(x)$   cdf of grain size distribution.
$h$   water height above the weir.
$k$   fitting parameter used in power regression between $L$ and $D$.
$L$   mean travel distance.
$p$   theoretical fitting parameter used in exponential particle size cdf.
$q$   fitting parameter used in power regression between $L$ and $D$.
$Q_b$   bed load transport rate.
$Q_{bf}$   sediment feed rate.
$Q_w$   water discharge.
$t$   experimental run duration.
$T_w$   temperature of the water.
$X_i$   measured travel distance of particles of size fraction $i$.

$x_{max}$ maximum possible travel distance.
$X$ theoretical travel distance.
$X'$ normalized theoretical travel distance.
$\alpha$ fitting parameter of the gamma distribution function of particle size.
$\beta$ fitting parameter of the gamma distribution function of particle size.
$\Gamma$ gamma function.
$\lambda$ fitting parameter of the exponential distribution function of travel distance.
$\mu$ mean of the normal random variable $\ln D$.
$\sigma$ standard deviation of the normal random variable $\ln D$.
$\rho_s$ solid particle density.
$\rho_w$ water density.
$\tau*$ nondimensionalized shear stress.
$\tau*_{ci}$ critical Shields stress.
$\tau_b$ bed shear stress.

# References

Aban, I. B., M. M. Meerschaert, and A. K. Panorska (2006), Parameter estimation methods for the truncated Pareto distribution, *J. Am. Stat. Assoc.*, *101*, 270–277.

Ancey, C., A. C. Davison, T. Böhm, M. Jodeau, and P. Frey (2008), Entrainment and motion of coarse particles in a shallow water stream down a steep slope, *J. Fluid Mech.*, *595*, 83–114.

Ashida, K., and M. Michiue (1972), Study on hydraulic resistance and bedload transport rate in alluvial streams (in Japanese), *Trans. Jpn. Soc. Civ. Eng.*, *206*, 59–69.

Ashworth, P. J., and R. I. Ferguson (1989), Size-selective entrainment of bed load in gravel bed streams, *Water Resour. Res.*, *25*, 627–634.

Benson, D. A., S. W. Wheatcraft, and M. M. Meerschaert (2000), The fractional-order governing equation of Lévy motion, *Water Resour. Res.*, *36*, 1413–1423.

Brummer, C. J., and D. R. Montgomery (2003), Downstream coarsening in headwater channels, *Water Resour. Res.*, *39*(10), 1294, doi:10.1029/2003WR001981.

Bunte, K., and S. R. Abt (2005), Effect of sampling time on measured gravel bed load transport rates in a coarse-bedded stream, *Water Resour. Res.*, *41*, W11405, doi:10.1029/2004WR003880.

Church, M., and M. A. Hassan (1992), Size and distance of travel of unconstrained clasts on a streambed, *Water Resour. Res.*, *28*, 299–303.

Church, M., and K. Rood (1983), Catalogue of alluvial river channel regime data, report, 99 pp., Dep. of Geogr., Univ. of B. C., Vancouver.

Cundall, P. A., and O. D. L. Strack (1979), A discrete numerical model for granular assemblies, *Géotechnique*, *29*, 47–65.

Dancey, C. L., P. Diplas, A. Papanicolaou, and M. Bala (2002), Probability of individual grain movement and threshold condition, *J. Hydraul. Eng.*, *128*, 1069–1075.

DellAngelo, L. (2007), Experimental study of different sized tracer particles in a gravel-bed laboratory flume, M. S. thesis, Univ. of Minn., Minneapolis.

Drake, T. G., and J. Calantoni (2001), Discrete particle model for sheet flow sediment transport in the nearshore, *J. Geophys. Res.*, *106*, 859–868.

Drake, T. G., R. L. Shreve, W. E. Dietrich, P. J. Whiting, and L. B. Leopold (1988), Bedload transport of fine gravel observed by motion-picture photography, *J. Fluid Mech.*, *192*, 193–217.

Einstein, H. A. (1937), Bedload transport as a probability problem (in German), Ph.D. thesis, ETH Zurich, Zürich, Switzerland. (English translation by W. W. Sayre in *Sedimentation*, edited by H. W. Shen, Appendix C, 105 pp., H. W. Shen, Fort Collins, Colo., 1972.)

Einstein, H. A. (1950), The bed-load function for sediment transportation in open channel flows, *Tech. Bull. 1026*, pp. 1–68, U.S. Dep. of Agric., Washington, D. C.

Engelund, F., and J. Fredsoe (1976), A sediment transport model for straight alluvial channels, *Nord. Hydrol.*, *7*, 293–306.

Feller, W. (1971), *An Introduction to Probability Theory and Its Applications*, vol. 2, 2nd ed., John Wiley, New York.

Ferguson, R. I., and S. J. Wathen (1998) Tracer-pebble movement along a concave river profile: Virtual velocity in relation to grain size and shear stress, *Water Resour. Res.*, *34*, 2031–2038.

Fernandez Luque, R., and R. van Beek (1976), Erosion and transport of bedload sediment, *J. Hydraul. Res.*, *14*, 127–144.

Ganti, V., M. M. Meerschaert, E. Foufoula-Georgiou, E. Viparelli, and G. Parker (2010), Normal and anomalous dispersion of gravel tracer particles in rivers, *J. Geophys. Res.*, *115*, F00A12, doi:10.1029/2008JF001222.

Garcia, M. H. (2008), Sediment transport and morphodynamics, Sedimentation engineering processes, measurements, modeling and practice, *ASCE Manual and Reports on Engineering Practice*, vol. 110, edited by M. Garcia, pp. 21–164, Am. Soc. of Civ. Eng., New York.

Gotoh, H., and T. Sakai (1997), Numerical simulation of sheetflow as granular material, *J. Waterw. Port Coastal Ocean Eng.*, *123*, 329–336.

Habersack, H. M. (2001), Radio-tracking gravel particles in a large braided river in New Zealand: A field test of the stochastic theory of bed load transport proposed by Einstein, *Hydrol. Processes*, *15*, 377–391.

Haff, P. K., and R. S. Anderson (1993), Grain scale simulations of loose sedimentary beds: The example of grain-bed impacts in aeolian saltation, *Sedimentology*, *40*, 175–198.

Haschenburger, J. K., and P. Wilcock (2003), Partial transport in a natural gravel bed channel, *Water Resour. Res.*, *39*(1), 1020, doi:10.1029/2002WR001532.

Hassan, M. A., M. Church, and A. P. Schick (1991), Distance of movement of coarse particles in gravel bed streams, *Water Resour. Res.*, *27*, 503–511.

Heald, J., I. McEwan, and S. Tait (2004), Sediment transport over a flat bed in a unidirectional flow: Simulations and validation, *Philos. Trans. R. Soc. London A*, *362*, 1973–1986.

Kalashnikov, V. (1997), *Geometric Sums: Bounds for Rare Events with Applications*, Kluwer Acad., Dordrecht, Netherlands.

Kellerhals, R., and D. I. Bray (1971), Sampling procedures for coarse fluvial sediments, *J. Hydraul. Div. Am. Soc. Civ. Eng.*, *97*, 1165–1180.

Kleinhans, M. G., and L. C. van Rijn (2002), Stochastic prediction of sediment transport in sand-gravel bed rivers, *J. Hydraul. Eng.*, *128*, 412–425.

Kodama, Y., H. Ikeda, and H. Iijima (1992), Longitudinal sediment sorting along a concave upward stream profile in a large flume (in Japanese), *Bull. Environ. Res. Cent.*, *16*, 119–123.

Kotz, S., T. J. Kozubowski, and K. Podgórski (2001), *The Laplace Distribution and Generalizations: A Revisit With Applications to Communications, Economics, Engineering, and Finance*, Birkhäuser, Boston.

Kozubowski, T. J., M. M. Meerschaert, and H.-P. Scheffler (2003), The operator nu-stable laws, *Publ. Math. Debrecen*, *63*(4), 569–585.

Lanzoni, S., and M. Tubino (1999), Grain sorting and bar instability, *J. Fluid Mech.*, *393*, 149–174.

Lisle, I. G., C. W. Rose, W. L. Hogarth, P. B. Hairsine, G. C. Sander, and J. Y. Parlange (1998), Stochastic sediment transport in soil erosion, *J. Hydrol.*, *204*, 217–230.

McEwan, I., M. Sorensen, J. Heald, S. Tait, G. Cunningham, D. Goring, and B. Willetts (2004), Probabilistic modeling of bed-load composition, *J. Hydraul. Eng.*, *130*, 129–139.

Meyer-Peter, E., and R. Müller (1948), Formulas for bed-load transport, in *Proceedings of the 2nd IAHR Meeting*, pp. 39–64, Madrid.

Miller, R. L., and R. J. Byrne (1966), The angle of repose for a single grain on a fixed bed, *Sedimentology*, *6*, 303–314.

Nikora, V., H. Habersack, T. Huber, and I. McEwan (2002), On bed particle diffusion in gravel bed flows under weak bed load transport, *Water Resour. Res.*, *38*(6), 1081, doi:10.1029/2001WR000513.

Paola, C., and R. Seal (1995), Grain size patchiness as a cause of selective deposition and downstream fining, *Water Resour. Res.*, *31*, 1395–1407.

Paola, C., G. Parker, R. Seal, S. K. Sinha, J. B. Southard, and P. R. Wilcock (1992), Downstream fining by selective deposition in a laboratory flume, *Science*, *258*, 1757–1760.

Papanicolaou, A. N., P. Diplas, N. Evaggelopoulos, and S. Fotopoulos (2002), Stochastic incipient motion criterion for spheres under various bed packing conditions, *J. Hydraul. Eng.*, *128*, 369–380.

Parker, G. (2008), Transport of gravel and sediment mixtures, Sedimentation engineering processes, measurements, modeling and practice, *ASCE Manual and Reports on Engineering Practice*, 110, M. Garcia, ed., chap. 3, pp. 165–252, Am. Soc. of Civ. Eng., New York.

Parker, G., and P. R. Wilcock (1993), Sediment feed and recirculating flumes: Fundamental difference, *J. Hydraul. Eng.*, *119*, 1192–1204.

Parker, G., C. M. Toro-Escobar, M. Ramey, and S. Beck (2003), Effect of floodwater extraction on mountain stream morphology, *J. Hydraul. Eng.*, *129*, 885–895.

Schmeeckle, M. W., and J. M. Nelson (2003), Direct numerical simulation of bedload transport using a local, dynamic boundary condition, *Sedimentology*, *50*, 279–301.

Schmeeckle, M. W., J. M. Nelson, and R. Shreve (2007), Forces on stationary particles in near-bed turbulent flows, *J. Geophys. Res.*, *112*, F02003, doi:10.1029/2006JF000536.

Schumer, R., and D. J. Jerolmack (2009), Real and apparent changes in sediment deposition rates through time, *J. Geophys. Res.*, *114*, F00A06, doi:10.1029/2009JF001266.

Shields, A. (1936), Anwendung der Aehnlichkeitsmechanik und der Turbulenzforschung auf die Geschiebebewegung (in German), Ph.D. theses, Mitteilungen der Preussiischen Versuchsanstalt f–r Wasserbau und Schiffhau, Heft 26, Berlin, Germany. (English translation by W.P. Ott and J.C. van Uchelen, *Rep. 167*, Hydrodyn. Lab., Calif. Inst. of Technol., Pasadena.)

Singh, A., K. Fienberg, D. J. Jerolmack, J. Marr, and E. Foufoula-Gergiou (2009), Experimental evidence for statistical scaling and intermittency in sediment transport rates, *J. Geophys. Res.*, *114*, F01025, doi:10.1029/2007JF000963.

Solari, L., and G. Parker (2000), The curious case of mobility reversal in sediment mixtures, *J. Hydraul. Eng.*, *126*, 185–197.

Southard, J. B. (1991), Experimental determination of bed-form stability, *Annu. Rev. Earth Planet. Sci.*, *19*, 423–455.

Stark, C. P., E. Foufoula-Georgiou, and V. Ganti (2009), A nonlocal theory of sediment buffering and bedrock channel evolution, *J. Geophys. Res.*, *114*, F01029, doi:10.1029/2008JF000981.

Straub, L. G. (1935), Some observations of sorting of river sediments, *Eos Trans. AGU*, *16*, 463–467.

Tsujimoto, T. (1978), Probabilistic model of the process of bedload transport and its application to mobile-bed problems, Ph.D. thesis, 174 pp., Kyoto Univ., Kyoto, Japan.

Vanoni, V. A., and N. H. Brooks (1957), Laboratory studies of the roughness and suspended load of alluvial streams, *Rep. E-68*, Sediment. Lab., Calif. Inst. of Technol., Pasadena.

Weeks, E. R., T. H. Solomon, J. S. Urbach, and H. L. Swinney (1998), Observation of anomalous diffusion and Lvy flights, in *Lvy Flights and Related Topics in Physics*, edited by M. F. Shlesinger et al., pp. 51–71, Springer, New York.

Wilcock, P. R., and J. B. Southard (1989), Bed-load transport of a mixed-size sediment: Fractional transport rates, bed forms, and the development of a coarse bed-surface layer, *Water Resour. Res.*, *25*, 1629–1641.

Wong, M., and G. Parker (2006), Reanalysis and correction of bed-load relation of Meyer-Peter and Müller using their own database, *J. Hydraul. Eng.*, *132*, 1159–1168.

Wong, M., G. Parker, P. DeVries, T. M. Brown, and S. J. Burges (2007), Experiments on dispersion of tracer stones under lower-regime plane-bed equilibrium bed load transport, *Water Resour. Res.*, *43*, W03440, doi:10.1029/2006WR005172.

L. DellAngelo, Barr Engineering, 4700 West 77th St., Ste. 200, Minneapolis, MN 55414, USA.

K. M. Hill, Saint Anthony Falls Laboratory, Department of Civil Engineering, University of Minnesota, Minneapolis, MN 55414, USA. (kmhill@umn.edu)

M. M. Meerschaert, Department of Statistics and Probability, Michigan State University, East Lansing, MI 48823, USA. (mcubed@stt.msu.edu)